1   Date: July 17, 2014

2   Submitted to: Atmospheric Chemistry and Physics

3   Revised manuscript

4

5

6   Estimation of the direct and indirect impacts of fireworks on the

7   physicochemical characteristics of atmospheric PM_{10} and $PM_{2.5}$

8

9   **Y.Z. Tian, J. Wang, X. Peng, G.L. Shi*, Y.C. Feng**

10 *State Environmental Protection Key Laboratory of Urban Ambient Air Particulate Matter*

11 *Pollution Prevention and Control, College of Environmental Science and Engineering, Nankai*

12 *University, Tianjin, 300071, China*

13

14

15

16

17

18

19

20

21 [*] Correspondence author. Tel.: +862223503397; fax: +862223503397.

22 E-mail address: nksgl@hotmail.com (G.-L. Shi).

23

Abstract:

To quantify the total, direct and indirect impacts of fireworks individually, size-resolved PM samples were collected before, during, and after a Chinese folk-custom festival (Chinese New Year) in a megacity in China. Through chemical analysis and morphological characterisation, a strong influence of fireworks on the physicochemical characteristics of PM_{10} and $PM_{2.5}$ was observed. The concentrations of many species exhibited an increasing trend during the heavy-firework period, especially for K^+, Mg^{2+} and Cr; and the results of the non-sea-salt ions demonstrated an anthropogenic influence on K^+ and Mg^{2+}. Then, source apportionment was conducted by receptor models and Peak Analysis. The total influence of the fireworks was quantified by PMF, showing that the fireworks contributed higher fractions (23.40% for PM_{10} and 29.66% for $PM_{2.5}$) during the heavy-firework period than during the light-firework period (4.28% for PM_{10} and 7.18% for $PM_{2.5}$). The profiles of the total fireworks obtained by two independent methods (PMF and peak analysis) were consistent, with higher abundances of K^+, Al, Si, Ca and OC. Finally, the individual contributions of the direct and indirect impacts of fireworks were quantified by CMB. The percentage contributions of resuspended dust, biomass combustion and direct fireworks were $36.82\pm8.37\%$%, $14.08\pm2.82\%$ and $44.44\pm8.26\%$, respectively, for PM_{10} and $34.89\pm4.19\%$, $16.60\pm3.05\%$ and $52.54\pm9.69\%$, respectively, for $PM_{2.5}$, in terms of the total fireworks. The quantification of the total, direct and indirect impacts of fireworks in the ambient PM

45   gives an original contribution to understand the physicochemical characteristics and

46   mechanisms of such high-intensity anthropogenic activities.

48

49

1 Introduction

Atmospheric particulate matter (PM) is recognised globally as a major environmental issue with adverse effects on air quality, regional visibility, global climate change and health effects (Ding et al., 2008; Robichaud and Ménard, 2014). By scattering and absorbing incoming solar radiation and outgoing terrestrial radiation directly, or by acting as cloud-condensation nuclei and thereby influencing the optical properties of clouds indirectly, atmospheric aerosols can influence the radiation balance of the earth's atmosphere (Lin et al., 2013; Shen et al., 2013). Ambient PM is a complex mixture of components from a variety of sources, including natural and anthropogenic sources (Zheng et al., 2005; Zhao et al., 2013a). In recent years, concerns about short-term air quality degradation events and their continuous negative effects to human health has increased, especially for PM pollution caused by high-intensity anthropogenic activities.

Firework displays are high-intensity anthropogenic activities that create notable air pollution and obvious short-term air-quality degradation. Firework displays are used to celebrate popular fiestas, a practice common worldwide (e.g., at the New Year). During firework episodes, there is usually a transient and spectacular increase in the PM pollution. Fireworks contain a variety of metal salts, such as chlorates and perchlorates (Wang et al., 2007; Crespo et al., 2012), leading to extremely high ambient concentrations of these species during the celebration. These heavy metals and perchlorates are all highly toxic (Shi et al., 2011) and are on average fine enough to be easily inhaled and show a health risk to susceptible individuals. Both the

72   long-term and short-term hazardous impacts of fireworks on human health have been

73   paid significant attention by researchers (Wang et al., 2007; Vecchi et al., 2008;

74   Crespo et al., 2012; Cheng et al., 2013).

75   Studies have demonstrated that the displacement of fireworks could be an

76   important source category for atmospheric PM (Vecchi et al., 2008). Fireworks can

77   influence the PM directly by emitting firework-related species (such as certain heavy

78   metals). Additionally, the accessory effects, which were indirectly caused by the

79   activities of firework displays, should be taken into consideration in the firework

80   events. For example, pyrotechnic device explosions can lead to resuspension of

81   materials already deposited on the ground; and biomass combustion (fireworks are

82   made from paper and a cracker) occurs when the fireworks are displayed and

83   incinerated after display. Although firework-related pollution episodes are transient in

84   nature, they are highly concentrated, and the influence is continuous. Both the direct

85   and indirect influences of fireworks might significantly contribute to PM and the total

86   annual metal emissions. However, the quantification of firework contributions,

87   especially for its direct and indirect impacts, is very limited.

88   Studies on fireworks have mainly applied the following methods: burning fireworks

89   in specific laboratories or fields to characterise their chemical properties (Tsai et al.,

90   2012); and investigating the environmental impacts through ambient sampling

91   champion during firework periods (Sarkar et al., 2010; Crespo et al., 2012). The

92   former cannot reflect the actual ambient condition and indirect impacts. For the latter,

93   celebrations by fireworks are usually continued for only a few days. Thus, it has been

94   very difficult to quantify the contributions of fireworks to ambient PM, especially for

95   the quantification of indirect impacts. Selecting an appropriate period and site for this

96   subject is key. Fireworks are more prevalent in certain places than others. China is the

97   country that produces the most fireworks in the world (Shi et al., 2011). In addition,

98   setting off fireworks is a traditional way to celebrate the Chinese New Year (CNY,

99   Spring Festival) and is justifiably welcomed all over the country. CNY is the most

100   important folk-custom holiday in China. Celebrations during CNY season tend to spill

101   over into the preceding and succeeding days (usually until the Lantern Festival,

102   another important festival in China), along with sporadic fireworks. During the

103   firework episodes, the anthropogenic emission patterns are greatly changed (Huang et

104   al., 2012). Many ordinary activities are decreased, such as certain industries and

105   traffic (Feng et al., 2012), whereas degradation of the air quality might occur due to

106   displays of fireworks. This provides a unique opportunity to study the drastic source

107   changes and allows the quantification of the direct and indirect contributions of

108   fireworks under significantly different emission patterns.

109   Therefore, the purpose of this work is to individually quantify the total, direct and

110   indirect contributions of fireworks to size-resolved PM. A sampling campaign of PM_{10}

111   and $PM_{2.5}$ was performed before, during, and after the CNY (as shown in Table S1) in

112   a megacity in China. The physicochemical characteristics of the PM during this

113   folk-custom festival were investigated, and the influence of fireworks on the

114   physicochemical changes was also studied. The tracer species of fireworks were

115   discussed and then used for the source identification. The total, direct and indirect

116   contributions of fireworks to PM were modelled using the Positive Matrix

117   Factorization (PMF), Peak Analysis (PA) and Chemical Mass Balance (CMB) models.

118   The quantitative assessment of the fireworks' direct and indirect impacts on the

119   ambient PM gives an original contribution to understand the physicochemical

120   characteristics and mechanisms during firework displays. The findings will aid in

121   studies on similar high-intensity anthropogenic activities.

122

123   **2 Methodology**

124   **2.1 Sampling**

125   The PM_{10} and $PM_{2.5}$ samples were collected in Tianjin (a megacity in China).

126   Tianjin, the largest harbour of Northern China, is a fast-growing and economically

127   developed city that has a population of more than 12 million and has more than 1.5

128   million automobiles. The air quality of Tianjin has declined with rapid urbanisation

129   and industrialisation. The sampling site is sited on the rooftop of a six-story building

130   that is located in a mixed residential and commercial area in Tianjin. Usually,

131   substantial degradation would occur during the firework displays in such a mixed area.

132   The map of the sampling site was indicated in Fig. S1.

133   The sampling campaign of PM_{10} and $PM_{2.5}$ was performed from 30 January 2013 to

134   24 February 2013, including periods before, during, and after the CNY (until the

135   Lantern Festival). The sampling periods and the corresponding Chinese lunar calendar

136   were listed in Table S1. During the sampling periods, firework displays occurred for

137   the celebration of the CNY holiday. For the period from CNY's Eve to the Lantern

138   Festival, fireworks are allowed in China, and numerous fireworks were consumed;

139   thus, this period is defined as a heavy-firework period. For the period before CNY's

140   Eve, sporadic fireworks might be set off, so it is defined as a light-firework period.

141   Based on our previous works and other related studies (Shi et al., 2009; Xue et al.,

142   2010; Harrison et al., 2012; Tian et al., 2013a; Zhao et al., 2013 a, b), the $PM_{2.5}$ and

143   PM_{10} were simultaneously collected on quartz-fibre filters and polypropylene-fibre

144   filters using medium-volume air samplers (TH-150) at a flow rate of 100 L/min. The

145   detailed information for the sampling and quality assurance/quality control (QA/QC)

146   are available in the Supplementary Materials.

147

148   **2.2 Chemical Analysis**

149   The elemental compositions (Al, Si, Ca, V, Cr, Mn, Fe, Co, Cu, Zn, As and Pb) of

150   the samples collected on the polypropylene-fibre filters were determined by

151   inductively coupled plasma-mass spectrometry (ICP-AES) (IRIS Intrepid II, Thermo

152   Electron). Ion chromatography (DX-120, DIONEX) was used to analyse the

153   water-soluble ions (NO_3^-, SO_4^{2-}, Na^+, K^+ and Mg^{2+}) collected on the quartz-fibre

154   filters. The organic carbon (OC) and elemental carbon (EC) concentrations of the

155   samples on the quartz-fibre filters were determined by DRI/OGC carbon analysis, a

156   technique based on the IMPROVE thermal/optical reflectance (TOR) protocol.

157   The background contamination was routinely monitored by blank tests. Enough

158   blank tests were conducted and used to valid and correct the corresponding data.

159   Certified reference materials (CRM, produced by National Research Center for

160 Certified Reference Materials, China) were used for quality assurance and quality

161 control. Blanks and duplicate sample analyses were performed for nearly 10% of the

162 samples. The pretreatment procedure, chemical analysis and QA/QC are described in

163 detail in the Supplementary Materials and refer to our previous works and other

164 related studies (Bi et al., 2007; Shi et al., 2009; Wu et al., 2009; Kong et al., 2010;

165 Xue et al., 2010; Zhao et al., 2013 a, b).

166 In addition, scanning electron microscopy (SEM) determinations were performed

167 by a JEOL JSM-7500F equipped with an X-ray energy dispersive spectrometer (EDS)

168 to perform a morphological characterisation and chemical analysis of the individual

169 particles.

170

171 **2.3 Modelling approaches**

172 **2.3.1 Receptor models**

173 Two widely used receptor models, Positive Matrix Factorisation (PMF) and

174 Chemical Mass Balance (CMB), were applied to quantify the total (sum of the direct

175 and indirect contributions), direct and indirect contributions of fireworks.

176 PMF is a useful factorisation methodology that can identify potential source

177 categories and source contributions when the source profiles are not known. It

178 identifies the source profile matrix F and quantifies the source contribution matrix G

179 based on observations at the receptor site (X). Following Paatro and Tapper (1994),

180 the PMF model can be represented in matrix form as:

181 $X = GF + E$, (1)

182　The elements of the source contribution matrix G and source profile matrix F are

183　constrained to non-negative values for PMF. PMF uses the residual matrix elements

184　(e_{ik}) and uncertainty estimates (σ_{ij}) to calculate a minimum Q value by using a

185　weighed least square method, which is defined as:

186　$$Q(E) = \sum_{i=1}^{m} \sum_{j-1}^{n} (e_{ij} / \sigma_{ij})^2,\qquad\qquad(2)$$

187　where σ_{ij} is the uncertainty of the jth species in the ith sample, which is used to weight

188　the observations that include sampling errors, detection limits, missing data, and

189　outliers (Paatero,2007). The goal of PMF is to minimise this function.

190　　PM data from the different sizes ($PM_{2.5}$ and PM_{10}) were combined and inputted into

191　PMF, as has been done in related works (Amato et al., 2009; Aldabe et al., 2011). The

192　combined data showed satisfactory results, and further analysis demonstrated that the

193　profiles of $PM_{2.5}$ and PM_{10} were similar in this work. Additionally, different numbers

194　of factors and different Fpeak values were considered and tested when running PMF.

195　The calculations were allowed to repeat ten times from ten pseudorandom starting

196　points for each computation, to test if a global minimum point was reached. The error

197　model code (EM=-14) and the uncertainties required for PMF were chosen according

198　to the user's guide (Paatero, 2007).

199　　Then, the CMB model was applied to quantify the individual contributions from the

200　direct and indirect impacts of fireworks. CMB is also a widely used receptor model,

201　for cases in which the number and profiles of sources are available (Watson et al.,

202　1984; Chen et al., 2012). Similar to PMF, the CMB can be described as:

203 $$x_{ij} = \sum_{p=1}^{p} g_{ip} f_{pj} + e_{ij} \qquad (3)$$

204 where x_{ij} is the jth species concentration measured in the ith sample; f_{pj} is the jth species

205 mass fraction in the pth source; g_{ip} is the contribution of the pth source to the ith sample;

206 and e_{ij} is the residual (Hopke,2003). In contrast to PMF, except for x_{ij}, f_{pj} should also

207 be available for the CMB model. USEPA CMB8.2 (USEPA, 2004) was applied in this

208 work. The main performance indices of CMB are the reduced chi square (χ^2), percent

209 mass (PM) and R square (R^2). Understanding the information of sources is important

210 for the CMB modelling. In this work, a field survey of sources was performed before

211 applying the CMB model, to determine the source categories.

212 **2.3.2 Peak Analysis**

213 In the present study, Peak Analysis was used to quantify the species abundances of

214 the fireworks based on the observations of the PM and chemical species. This method

215 was successfully applied to determine the profiles of the vehicle emissions (Ke et al.,

216 2013). The highest and lowest PM or species concentrations were used to represent

217 the peak and background observations, respectively. The peak period had the strongest

218 fireworks density, whereas the background values corresponded to the lowest

219 fireworks density. Then, the species abundances were obtained by normalising their

220 concentrations with the corresponding PM concentrations, as follows (Ke et al, 2013):

221 $$F_j = \frac{c_{p,j} - c_{b,j}}{c_{p,PM} - c_{b,PM}}, \qquad (4)$$

222 where F_j is the abundance (g per g of PM) for the jth species, $C_{p,j}$ and $C_{b,j}$ are the jth

223 species concentrations ($\mu g/m^3$) in the peak observation and the background

224   observation, respectively; and $C_{p, PM}$ and $C_{b, PM}$ are the PM concentrations ($\mu g/m^3$) in

225   the peak and the background observations, respectively.

226   The uncertainty (σ_{F_j}) of the jth species abundance (F_j) was defined as follows (Ke

227   et al, 2013):

228   $$\sigma_{F_j} = F_j \sqrt{(\frac{\sigma_{p,j}}{c_{p,j}})^2 + (\frac{\sigma_{b,j}}{c_{b,j}})^2} \,, \qquad\qquad (5)$$

229   where $\sigma_{p,j}$ and $\sigma_{b,j}$ are the measurement uncertainties ($\mu g/m^3$) of the jth species in

230   the peak observation and the background observation, respectively. The results of the

231   Peak Analysis method were employed to describe the profiles of the total fireworks.

232

233   **3 Results and discussion**

234   **3.1 Physicochemical characteristics of PM$_{10}$ and PM$_{2.5}$**

235   The PM samples were acquired on two filters for each sampling day, so consistency

236   tests play an important role in the QA/QC process. The comparisons between the

237   concentrations measured on the polypropylene-fibre filters and those on the

238   quartz-fibre filters were shown in Fig. S2. A satisfactory consistency (slopes close to

239   unity and high correlations) were observed, indicating good quality assurance.

240   Because the quartz-fibre filters tend to absorb water and be shredded during sampling

241   handling (Cheng et al., 2011), concentrations on the polypropylene-fibre filters were

242   used in the following discussion.

243   The concentrations of the PM$_{10}$ and PM$_{2.5}$ in Tianjin during the sampling periods

244   are summarised in Fig. S3. The average concentration of PM$_{10}$ was 212.95 $\mu g/m^3$, and

245   that of PM$_{2.5}$ was 140.59 $\mu g/m^3$, with an average ratio of PM$_{2.5}$/ PM$_{10}$ of 0.66. The

12

246     $PM_{2.5}/ PM_{10}$ values were 0.65 and 0.66 during the light-firework and heavy-firework

247   periods, respectively. The T-test was used to analyse the difference between the

248     $PM_{2.5}/ PM_{10}$ values in the two periods, and the results indicated an insignificant

249   difference with p>0.05. The PM_{10} and $PM_{2.5}$ concentrations were 148.74 μg/m^3 and

250   96.80 μg/m^3, respectively, during the light-firework period and 249.08 μg/m^3 and

251   165.23 μg/m^3, respectively, during the heavy-firework period. The highest

252   concentrations were observed on CNY's Eve, when massive firework displays usually

253   occur all over the country (Feng et al., 2012), indicating the huge influence of

254   fireworks on the PM concentrations. According to the previous studies, the ambient

255   PM_{10} concentrations of Tianjin in the winter of 2000 was 177.78 ug/m^3 on average

256   which was higher than 148.74 μg/m^3 (during light--firework periods), lower than

257   249.08 μg/m^3 (during heavy-firework periods) (Tian et al., 2013b). The ambient $PM_{2.5}$

258   concentrations of Tianjin in winter 2008 was 227.2 ug/m^3 on average (Kong et al.,

259   2010) which was higher than the 96.8 μg/m^3 (during light--firework periods) and

260   165.23μg/m^3 (during heavy-firework periods).

261   The study of the chemical composition is critical for understanding the

262   physicochemical characteristics of pollution during the folk-custom festival. The

263   average concentrations of the chemical species in PM_{10} and $PM_{2.5}$ during the

264   light-firework period and the heavy-firework period were exhibited in Fig. 1, and the

265   abundance of the species (fractions of the species in PM) in PM_{10} and $PM_{2.5}$ were

266   summarised in Fig. S4. According to Fig. 1 and Fig. S4, the crustal elements (Al, Si,

267   Fe, and Ca), carbonaceous species (OC and EC) and several water-soluble ions (Cl$^-$,

268   NO_3^- and SO_4^{2-}) were important species in PM_{10} and $PM_{2.5}$ during the sampling

269   periods. The concentrations of OC were 9.84 and 15.58 μg/m³ in PM_{10} and were 7.61

270   and 11.32 μg/m³ in $PM_{2.5}$ during the light- and heavy-firework periods, respectively.

271   The concentrations of EC were 5.59 (in PM_{10} during the light-firework period), 6.79

272   (in PM_{10} during the heavy-firework period), 4.20 (in $PM_{2.5}$ during the light-firework

273   period) and 4.55 (in $PM_{2.5}$ during the heavy-firework period) μg/m³. The ratio of

274   OC/EC was higher during the heavy-firework period for both PM_{10} and $PM_{2.5}$, with

275   values of 1.76 (light-firework) and 2.32 (heavy-firework) for PM_{10} and 1.81

276   (light-firework) and 2.49 (heavy-firework) for $PM_{2.5}$. Additionally, it was interesting

277   to find that K^+ played an important role during the heavy-firework period, in contrast

278   to its effect during the light-firework period. Compared with prior studies (Kong et al.,

279   2010; Tian et al., 2013b), several differences can be observed in chemical

280   compositions.

281   **(Fig. 1)**

282   In addition, for further characterisation, images and micrographs of the quartz-fibre

283   filters were exhibited. Fig. S5 shows photos of the quartz filters with the PM_{10} and

284    $PM_{2.5}$ samples for two cases: a normal day in the light-firework period and CNY's

285   Eve in the heavy-firework period. A difference can be observed between the filters.

286   Furthermore, Fig. S6 shows micrographs of $PM_{2.5}$ for the same days. There were

287   many more particles for the samples from CNY's Eve than for those from the normal

288   day, demonstrating the much higher concentration levels on CNY's Eve.

289

3.2 Influence of fireworks on the physicochemical characteristics of PM pollution

Comparing the mass concentrations and abundances of species during the heavy-firework period with those during the light-firework period could help researchers learn more about the influence of this intensive human activity. As shown in Fig. 1, concentrations of most species (such as crustal elements, heavy metal species, carbonaceous species, Cl^-, Na^+, K^+, and Mg^{2+}) exhibited increasing trends during the heavy-firework period. It is believed that Al, Ca, Cr, Cu, Pb, Cl^-, Na^+, K^+, and Mg^{2+} might represent firework-related species. Potassium is one of the major components of fireworks because potassium compounds in black powder (commonly in the form perchlorate or chlorate) act as the main oxidisers during burning, with the corresponding chemical equations being $2KClO_3=2KCl+3O_2$ and $KClO_4=KCl+2O_2$. Ca compounds (such as calcium chloride and sulphate) and Cu compounds (such as copper chloride and oxide) give rise to orange and blue colourations, respectively. A Cr compound ($CuCr_2O_4$) is used as a catalyst for propellants. Cu, K, and Cr are used to provide silvery and glitter effects as well. Mg is a useful metallic fuel and is also used to produce sparks and crackling stars (in the form of the 50:50 Mg:Al alloy magnalium). Al also can be used alone as a common constituent for fuel, sparks and glitter effects. Pb can help to achieve steady and reproducible burning rates. Many components are in the form of perchlorate or chlorate, leading to high concentrations of Cl^-. The abruptly high emissions of these elements due to firework combustion can explain the high concentrations of these firework-related species in atmospheric PM during the heavy-firework period. It is noteworthy that certain firework-related heavy

312   metals (Cr, Pb, Cu, etc.) are dangerous elements because of their toxicity and are

313   forbidden by law in many countries. Such high concentrations in a short time,

314   especially in a place where a considerable number of people are gathered, might be of

315   concern.

316   Except for the directly firework-related species, an increase was also observed for

317   most of the crustal elements (such as Al, Si and Ca). Although Al and Ca might derive

318   from industrial and direct firework sources, the abrupt increase of crustal elements

319   might also be due to the resuspension of materials already deposited on the ground,

320   caused by pyrotechnic device explosions. Additionally, higher concentrations of K^+

321   and OC, which are good markers of biomass combustion, might imply the

322   contribution of biomass combustion during the heavy-firework period. The higher

323   concentrations of these indirect markers during the heavy-firework period can be

324   ascribed partly to the indirect influence of fireworks. The important contributions of

325   the resuspended dust and biomass combustion must be taken into consideration as

326   sources of PM in these firework events. Moreover, the mass ratios of NO_3^- to SO_4^{2-}

327   (NO_3^-/SO_4^{2-}) during the heavy-firework period were lower than the ratios during the

328   light-firework period. Similarly, lower NO_3^-/SO_4^{2-} during CNY was observed in

329   Beijing (Feng et al., 2012). The change in NO_3^-/SO_4^{2-} might be partly due to differing

330   formation mechanisms. Wang et al. (2007) reported the dominance of metal-catalysed

331   heterogeneous formation of sulphate during the firework period. Goodman et al.

332   (2001) reported a different formation mechanism for nitrate. However, the formation

333   of secondary particles might be influenced by considerable factors (such as

334   meteorological conditions and precursors) and is very complex.

335   Some of the species mentioned here require further study. SEM micrographs and

336   EDS spectra of particles on the normal day and on CNY's Eve were exhibited in Fig.

337   S7. The individual-particle analysis showed a higher K level on CNY's Eve than on

338   the normal day. Furthermore, K^+, Cr, and Mg^{2+} particularly stand out as species that

339   have far higher concentrations during the heavy-firework period than that during the

340   light-firework period. The H/L values (the ratios of the concentrations in the

341   heavy-firework period to those in the light-firework period) of the K^+, Cr, and Mg^{2+}

342   concentrations were 6.29, 5.52, 3.97 for PM_{10} and 5.78, 4.63, 6.32 for $PM_{2.5}$ (as shown

343   in Fig. 1), respectively. The mass concentrations may not completely reflect the

344   composition of PM, so a comparison of the species abundances was also performed.

345   As shown in Fig. S4, the abundances of K^+, Cr, and Mg^{2+} were obviously higher

346   during the heavy-firework period, with H/L values of 3.08, 4.44, 1.78 for PM_{10} and

347   2.68, 2.06 and 2.37 for $PM_{2.5}$, respectively. The high H/L values of the abundances

348   can demonstrate the intensive influence of the fireworks on these species. For further

349   investigation, the daily variations in the concentrations and abundances of the most

350   firework-influenced species (K^+, Mg^{2+} and Cr) were shown in Fig. S8. Similar

351   temporal patterns were observed for these species. Both the mass concentrations and

352   abundances of K^+, Mg^{2+} and Cr showed sharp peaks for CNY's Eve for $PM_{2.5}$ and

353   PM_{10}. Obvious increases also occurred on the fifth day of the Chinese lunar calendar

354   and the Lantern Festival, which are important folk-custom days for fireworks. Thus,

355   K^+, Mg^{2+} and Cr could indicate the influence of fireworks, which is important for

356   further identification of the source categories of fireworks.

357   Species in PM may result from anthropogenic and natural sources. To focus the

358   characteristics of anthropogenic emissions, the non-sea-salt (nss) ions were calculated.

359   Assuming that all of the Na^+ ions were from sea salt, the concentrations of $nss\text{-}SO_4^{2-}$,

360    $nss\text{-}Cl^-$, $nss\text{-}K^+$ and $nss\text{-}Mg^{2+}$ in PM_{10} and $PM_{2.5}$ were calculated based on the

361   composition of average seawater. The relative mass concentrations of SO_4^{2-}, Cl^-, K^+

362   and Mg^{2+} to Na^+ are 0.252, 1.8, 0.037 and 0.119, respectively (Feng et al., 2012).

363   Nearly all SO_4^{2-} and K^+ (>98%) and most Mg^{2+} (>75%) ion in both PM_{10} and $PM_{2.5}$

364   are from non-sea-salt. It is interesting to find a higher percentage of $nss\text{-}Cl^-$ in $PM_{2.5}$

365   (72%) than in PM_{10} (57%), indicating the stronger influence of anthropogenic

366   emissions on the Cl^- in fine PM. This result is reasonable because sea salt contributes

367   a higher fraction to the coarse fraction of PM (Keuken et al., 2013). To investigate the

368   anthropogenic impacts of fireworks, a comparison was conducted between nss-ions

369   during the light-firework and heavy-firework periods. The $nss\text{-}SO_4^{2-}$ accounts for

370   more than 98% of the SO_4^{2-} in both the $PM_{2.5}$ and PM_{10}, and there was no obvious

371   difference (p > 0.05) during the two periods. The concentrations of $nss\text{-}Cl^-$, $nss\text{-}K^+$

372   and $nss\text{-}Mg^{2+}$ as well as their percentages in the total ions were exhibited in Fig. S9.

373   For these three ions, much higher concentrations and higher percentages occurred

374   during the heavy-firework period, especially on CNY's Eve, with more than 88% of

375   the ions resulting from anthropogenic impacts. These results suggest the large

376   anthropogenic influence on Cl^-, K^+, Mg^{2+}, which may be mainly caused by fireworks

377   during the Chinese folk-custom festival; as a result, they were effective to indicate the

378 presence of fireworks. In the present work, the sources to Cl⁻ are complex, including

379 not only anthropogenic but also natural sources (Vassura et al., 2014). Additionally,

380 considering insufficient concentrations of Cr in the PM mass, K^+ and Mg^{2+} may be

381 more powerful as tracers of fireworks for the following source apportionment, as

382 indicated by related reports (Wang et al., 2007; Cheng et al., 2013).

383

384 **3.3 Sources of PM**

385 To quantitatively evaluate the total, direct and indirect impacts of fireworks on

386 ambient PM, source apportionment of size-resolved PM samples was modelled by the

387 PMF, Peak Analysis and CMB models in this section.

388 **3.3.1 Total contributions of fireworks by PMF modelling**

389 PMF was first applied to identify the possible source categories and to quantify

390 their contributions to PM during the sampling periods. By checking the variation in

391 the Q values and the model performance, the five-factor solution and Fpeak=0.1 were

392 determined for fitting. The fitting plot between the measured and estimated PM

393 concentrations was exhibited in Fig. S10. The slope of the regression was 0.96, and

394 the Pearson correlation coefficient was 0.98, suggesting perfect performance of PMF

395 in this run (the estimated PM concentrations for most samples were similar to the

396 measured concentrations).

397 The source profiles obtained by PMF are listed in Fig. 2 and Table S2. According

398 to Fig. 2, Factor 1 exhibited high loadings for Al, Si, Ca, etc., which are associated

399 with crustal dust (Pant and Harrison et al., 2012). In Factor 2, relatively higher

400 loadings of Al, Si and OC were observed. Previous studies demonstrated that

401 simultaneously high Al, Si and OC might indicate coal combustion as the source

402 category (Zhang et al., 2011; Pant and Harrison et al., 2012). Factor 3 correlates

403 strongly with SO_4^{2-} and NO_3^-, consistent with source categories related to secondary

404 particles (secondary sulphate and secondary nitrate) (Gao et al., 2011; Tian et al.,

405 2013a). Factor 4 is mainly characterised by OC and EC, which were indicative of

406 vehicular exhaust (Pant and Harrison et al., 2012). The percentage contributions of

407 these source categories were summarised in Fig. 2 as well.

408 **(Fig. 2)**

409 In Factor 5, K^+ presented obviously high weightings. As discussed above, K^+ may

410 be a tracer of fireworks, and the higher loading of Mg^{2+} in this factor might also

411 indicate the impacts of fireworks. Furthermore, it is interesting to find the relatively

412 higher weightings of other species, such as OC, Al, Si and Ca. Strong links with K^+

413 and OC could demonstrate biomass combustion (Cheng et al., 2013). Factor 5 was

414 also associated with Al, Si and Ca, which are crustal elements. Biomass combustion

415 might be indirectly caused by fireworks, which can occur when the fireworks are

416 displayed and incinerated after display. Crustal elements might result from the

417 resuspension of materials already deposited on the ground (caused by pyrotechnic

418 device explosions). Therefore, Factor 5 represented the total influence of fireworks,

419 which might include the direct-firework contribution and indirect impacts (biomass

420 combustion and resuspended dust). PMF extracts source profiles and quantifies

421 contributions based on the temporal variation of the chemical species, so source

422 categories in one emission pattern might be identified as one factor. In this work,

423 direct fireworks, resuspended dust and biomass combustion caused by fireworks may

424 have similar emission patterns.

425   As exhibited in Fig. 2, the total influence of fireworks, including the direct-firework

426 and indirect impacts, contributed 19.29% to PM_{10} and 24.09% to $PM_{2.5}$ during the

427 entire sampling periods. The averaged percentage source contributions to PM_{10} and

428 $PM_{2.5}$ during the light-firework and heavy-firework periods, respectively, are

429 calculated and shown in Fig. 3. A large difference can be observed. During the

430 light-firework period, the total influence of fireworks contributed 4.28% to PM_{10} and

431 7.18% to $PM_{2.5}$; while during the heavy-firework period, the total influence of the

432 fireworks increased to rather high fractions (23.40% for PM_{10} and 29.66% for $PM_{2.5}$).

433 The time series of the percentage contributions of the total firework impacts on PM_{10}

434 and $PM_{2.5}$ were exhibited in Fig. 4, which could represent the trend of the total

435 firework impacts (including direct fireworks, resuspended dust and biomass

436 combustion). The most significant peak of the total firework contributions was

437 presented on CNY's Eve, indicating the heavy impacts of the total fireworks on this

438 day, although the contributions may be overestimated due to the uncertainties in the

439 results by PMF. In most cities in China, fireworks are allowed from CNY's Eve to the

440 Lantern Festival (namely, the heavy-firework period in this work). Numerous

441 fireworks were displayed on the night of CNY's Eve, as it is the most important

442 celebration of the year. Another peak of firework contributions was observed on the

443 Lantern Festival. The Lantern Festival is also an important festival in China and is the

444 last day that fireworks are allowed. The variation in the firework contributions was

445 consistent with the Chinese folk celebrations, which demonstrate the good

446 performance of PMF for modelling the total firework contributions in this work.

447   **(Fig. 3)**

448   **(Fig. 4)**

449 **3.3.2 Species abundances of the total firework impacts**

450   In addition to PMF, Peak Analysis was also employed to better understand the total

451 firework impacts. As discussed above, the profiles and contributions of the total

452 firework impacts were determined by PMF for PM_{10} and $PM_{2.5}$. Furthermore, Peak

453 Analysis (Ke et al., 2013) was employed in this section to investigate the species

454 abundances of the total fireworks in terms of the observations. The species

455 abundances of the total firework impacts obtained by the two independent methods

456 (PMF and Peak Analysis) were exhibited in Fig. 5. Considering the complexity

457 mentioned previously, the secondary ions were not included in the comparison.

458 Comparing the firework profiles, the abundances of most chemical species by Peak

459 Analysis were similar to the corresponding values by PMF. As shown in Fig. 5, the

460 abundance of K^+, which is the main marker of direct-fireworks as discussed above,

461 were consistent in the three firework profiles, with values of 16.34% by PMF, 15.21%

462 by Peak Analysis for PM_{10} and 17.33% by Peak Analysis for $PM_{2.5}$. The Al, Si and Ca

463 (resuspended dust elements) as well as OC (marker of biomass combustion along with

464 K^+) levels were also in agreement. The abundances of Al were 5.87%, 6.72% and

465 7.02%; Si were 9.87%, 10.07% and 11.85%; and OC were 6.32%, 5.87% and 6.60%,

466   estimated by PMF, by Peak Analysis for PM_{10} and by Peak Analysis for $PM_{2.5}$,

467   respectively. For a further investigation of the similarity among these profiles,

468   regression analyses and correlation coefficients (R) were computed and shown in Fig.

469   5. It is visible from Fig. 5 that all of the correlation coefficients were greater than 0.9,

470   suggesting that the total firework profiles obtained by PMF and by Peak Analysis

471   were concordant. In addition, the firework profiles of $PM_{2.5}$ were similar with those of

472   PM_{10}, implying that it is reasonable to introduce the combined dataset of $PM_{2.5}$ and

473   PM_{10} into PMF.

474   **(Fig. 5)**

475   **3.3.3 Contributions of the direct and indirect firework impacts**

476   As discussed above, the total influence of the fireworks might include indirect

477   impacts (resuspended dust and biomass combustion) and direct-fireworks. Thus, it is

478   necessary to deeply evaluate the individual impacts of fireworks. In this work, the

479   total firework profiles calculated by Peak Analysis were applied as the receptors in

480   the CMB model, and the source profiles of three contributors (resuspended dust,

481   biomass combustion and direct-fireworks) were incorporated into the model, to

482   individually determine the direct and indirect impacts of fireworks. In this work, the

483   source profiles of the resuspended dust were from our prior works in Tianjin (Zhang

484   et al., 2011); the biomass combustion profiles were from speciate 4.0 of the US EPA;

485   and the firework profiles were taken from a reported work (Tsai et al., 2012). The

486   performance indices of CMB in this work were summarised in Table S3. The values

487   of the performance indices met the requirement, indicating that the results of CMB

488   might be reliable.

489   The individual contributions to the total firework impacts (based on Peak Analysis)

490   were exhibited in Fig. 3 and Table S3. According to the estimations, the percentage

491   contributions of resuspended dust, biomass combustion and direct-fireworks were

492    $36.82 \pm 8.37\%$, $14.08 \pm 2.82\%$ and $44.44 \pm 8.26\%$, respectively, for PM_{10}, accounting for

493   the total firework contribution. For $PM_{2.5}$, the percentage contributions were estimated

494   to be $34.89 \pm 4.19\%$ from resuspended dust, $16.60 \pm 3.05\%$ from biomass combustion,

495   and $52.54 \pm 9.69\%$ from direct-fireworks. The sum of resuspended dust, biomass

496   burning and direct-fireworks was >100% for $PM_{2.5}$ and < 100% for PM_{10}, however,

497   they were in the range of the 80-120%, which met the requirement of the CMB. The

498   results demonstrated that fireworks can lead to a comprehensive influence on the

499   ambient PM. In addition to the direct-firework influence, resuspended dust and

500   biomass combustion indirectly caused by fireworks should also be considered.

501

502   **4 Conclusions**

503   To quantify the total, direct and indirect impacts of fireworks, size-resolved PM

504   samples were collected in a megacity in China. The sampling campaign covered a

505   Chinese folk-custom festival (CNY), which provides a unique opportunity to quantify

506   the contributions of fireworks under significantly different emission patterns. The

507   strong influence of fireworks on the physicochemical characteristics of atmospheric

508   PM_{10} and $PM_{2.5}$ was observed. The highest PM concentrations were observed on

509   CNY's Eve, when massive firework displays usually take place all over the country.

The concentrations of most species (such as crustal elements, heavy metal species, carbonaceous species, Cl^-, Na^+, K^+, and Mg^{2+}) exhibited increased trends during the heavy-firework period. Among these, K^+, Mg^{2+} and Cr showed the most obvious increase, and the results of non-sea-salt ions demonstrated the anthropogenic influence on these species. K^+, Mg^{2+} and Cr can be good tracers for fireworks, especially for K^+ and Mg^{2+}, which had higher concentrations. Subsequently, source apportionment was conducted using receptor models. The total influence of fireworks was quantified by PMF, contributing higher fractions during the heavy-firework period than those during the light-firework period. The profiles of the total fireworks obtained by PMF and Peak Analysis were consistent, with higher abundances of K^+, Al, Si, Ca and OC. Finally, the individual contributions of the direct and indirect impacts of fireworks were determined by the CMB model based on profiles from Peak Analysis. The present study demonstrated that fireworks might lead to a comprehensive influence on the ambient PM. Both the direct influence and indirect impacts (resuspended dust and biomass combustion) caused by fireworks should be considered. The present work can be helpful in understanding the physicochemical characteristics and mechanisms of such high-intensity anthropogenic activities.

532   Laboratory of the Tianjin Meteorological Bureau.

533

534   **References**

535   Aldabe, J., Elustondo, D., Santamar á, C., Lasheras, E., Pandolfi, M., Alastuey, A.,

536   Querol, X., and Santamar á, J.M.: Chemical characterisation and source

537   apportionment of PM2.5 and PM10 at rural, urban and traffic sites in Navarra

538   (North of Spain), Atmos. Res., 1, 191-205, 2011.

539   Amato, F., Pandolfi, M., Escrig, A., Querol, X., Alastuey, A., Pey, J., Perez, N., and

540   Hopke, P. K.: Quantifying road dust resuspension in urban environment by

541   multilinear engine: a comparison with PMF2, Atmos. Environ., 17, 2770-2780,

542   2009.

543   Bi, X.H., Feng, Y.C., Wu, J.H., Wang, Y.Q., and Zhu, T.: Source apportionment of

544   PM10 in six cities of northern China, Atmos. Environ., 41, 903-912, 2007.

545   Chen, W.A., Watson, J.G., Chow, J.C., Green, M.C., Inouye, D., and Dick, K.:

546   Wintertime particulate pollution episodes in an urban valley of the Western US: a

547   case study, Atmos. Chem. Phys., 12, 10051-10064, 2012.

548   Cheng, Y., Engling, G., He, K.B., Duan, F.K., Ma, Y.L., Du, Z.Y., Liu, J.M ., Zheng,

549   M., and Weber, R.J.: Biomass burning contribution to Beijing aerosol, Atmos.

550   Chem. Phys., 13, 7765-7781, 2013.

551   Cheng, Y., Zou, S.C., Lee, S.C., Chow, J.C. , Ho, K.F., Watson, J.G. , Han, Y.M.,

552   Zhang, R.J., Zhang, F., Yau, P.S., Huang , Y., Bai, Y. , and Wu, W.J.: Characteristics

553   and source apportionment of PM1 emissions at a roadside station, J. Hazard. Mater.,

554   195, 82-91, 2011.

555   Crespo, J., Yubero, E., Nicolás, J.F., Lucarelli, F., Nava, S., Chiari, M., Calzolai, G.:

556   High-time resolution and size-segregated elemental composition in high-intensity

557   pyrotechnic exposures, J. Hazard. Mater., 241-242, 82-91, 2012.

558   Ding, X., Zheng, M., Yu, L.P., Zhang, X.L., Weber, R.J., Yan, B., Russell, A.G.,

559   Edgerton, E.S., and Wang, X.M.: Spatial and Seasonal Trends in Biogenic

560   Secondary Organic Aerosol Tracers and Water-Soluble Organic Carbon in the

561   Southeastern United States, Environ. Sci. Technol, 42, 5171-5176, 2008.

562   Feng, J.L., Sun, P., Hu, X.L., Zhao, W., Wu, M.H., and Fu, J.M.: The chemical

563   composition and sources of PM 2.5 during the 2009 Chinese New Year's holiday in

564   Shanghai, Atmos. Res., 118, 435-444, 2012.

565   Gao, X., Yang, L., Cheng, S., Gao, R., Zhou, Y., and Xue, L.: Semi-continuous

566   measurement of water-soluble ions in PM 2.5 in Jinan, China: temporal variations

567   and source apportionments, Atmos. Environ., 45, 6048-6056, 2011.

568   Goodman, A.L., Bernard, E.T., and Grassian, V.H.: Spectro-scopic study of nitric acid

569   and water adsorption on oxide particles: enhanced nitric acid uptake kinetics in the

570   presence of adsorbed water, J. Phys. Chem. A, 105 (26), 6443-6457, 2001.

571   Hopke, P. K.: Recent developments in receptor modeling, J. Chemom., 17, 255-265,

572   2003.

573   Huang, K., Zhuang, G., Lin, Y., Wang, Q., Fu, J.S., Zhang, R., Li, J., Deng, C., and Fu,

574   Q.: Impact of anthropogenic emission on air quality over a megacity − revealed

575   from an intensive atmospheric campaign during the Chinese Spring Festival, Atmos.

576   Chem. Phys., 12, 11631–11645, 2012.

577   Ke, H.H., Ondov, J.M., and Rogge, W.F.: Detailed emission profiles for on-road

578   vehicles derived from ambient measurements during a windless traffic episode in

579   Baltimore using a multi-model approach, Atmos. Environ., 81, 280-287, 2013.

580   Keuken, M.P., Moerman, M., Voogt, M., Blom, M., Weijers, E.P., Röckmann , T., and

581   Dusek, U.: Source contributions to PM2.5 and PM10 at an urban background and a

582   street location, Atmos. Environ.,71, 26-35 ,2013.

583   Kong, S.F., Han, B., Bai, Z.P., Chen, L. Shi, J.W., and Xu, J.W.: Receptor modeling of

584   PM2.5, PM10 and TSP in different seasons and long-range transport analysis at a

585   coastal site of Tianjin, China, Sci. Total Environ., 408, 4681–4694, 2010.

586   Lin, Z. J. , Tao, J. , Chai, F. H., Fan, S. J., Yue, J. H., Zhu, L. H. , Ho, K. F.,and Zhang,

587   R. J.: Impact of relative humidity and particles number size distributionon aerosol

588   light extinction in the urban area of Guangzhou, Atmos. Chem. Phys., 13,

589   1115-1128, 2013.

590   Paatero, P., Tapper, U.: Positive Matrix Factorization: a non-negative factor model

591   with optimal utilization of error estimates of data values, Environmetrics, 5,

592   111-126, 1994.

593   Paatero, P.: User's guide for positive matrix factorization programs PMF2 and PMF3,

594   part 1-2: tutorial. Helsinki, Finland: University of Helsinki, 2007.

595   Pant, P., and Harrison, R.M.: Critical review of receptor modelling for particulate

596   matter: A case study of India, Atmos. Environ., 49, 1-12, 2012.

597   Robichaud, A. and Ménard, R.: Multi-year objective analyses of warm season

598   ground-level ozone and PM 2.5 over North America using real-time observations

599   and Canadian operational air quality models, Atmos. Chem. Phys., 14, 1769−1800,

600   2014.

601 Sarkar, S., Khillare, P.S., Jyethi, D.S., Hasan, A., Parween, M.: Chemical speciation of

602   respirable suspended particulate matter during a major firework festival in India. J.

603   Hazard. Mater., 184, 321−330, 2010.

604 Shen, G.F., Tao, S., Wei, S.Y., Chen, Y.C., Zhang, Y.Y., Shen, H.Z., Huang, Y., Zhu, D.,

605   Yuan, C.Y., Wang, H.C., Wang, Y.F., Pei, L.J., Liao, Y. L., Duan, Y.H., Wang, B.,

606   Wang, R., Lv, Y., Li, W., Wang, X.L., and Zheng, X.Y.: Field Measurement of

607   Emission Factors of PM, EC, OC, Parent, Nitro‑, and Oxy- Polycyclic Aromatic

608   Hydrocarbons for Residential Briquette, Coal Cake, and Wood in Rural Shanxi,

609   China, Environ. Sci. Technol, 47, 2998−3005, 2013.

610 Shi, G.L., Feng, Y.C., Zeng, F., Li, X., Zhang, Y.F., and Wang, Y.Q.: Use of a

611   Nonnegative Constrained Principal Component Regression Chemical Mass Balance

612   Model to Study the Contributions of Nearly Collinear Sources, Environ. Sci.

613   Technol, 43, 8867-73, 2009.

614 Shi, Y.L., Zhang, N., Gao, J.M., Li, X., Cai, Y.Q.: Effect of fireworks display on

615   perchlorate in air aerosols during the Spring Festival, Atmos. Environ., 45,

616   1323-1327, 2011.

617 Tian, Y.Z., Shi, G.L., Han, S.Q., Zhang, Y.F., Feng, Y.C., Liu, G.R., Gao, L.J., Wu, J,H.,

618   and Zhu, T.: Vertical characteristics of levels and potential sources of water-soluble

619   ions in PM10 in a Chinese megacity, Sci. Total Environ., 447, 1-9, 2013a.

Tian, Y.Z., Xiao, Z.M., Han, B., Shi, G.L., Wang, W., Hao, H.Z., Li, X., Feng, Y.C.,

and Zhu, T: Seasonal Study of Primary and Secondary Sources of Carbonaceous

Species in PM10 from Five Northern Chinese Cities, Aerosol Air Qual. Res., 13,

148–161, 2013b.

Tsai, H.H., Chien, L.H., Yuan, C.S., Lin, Y.C., Jen, Y.H., and Ie, I.R.: Influences of

fireworks on chemical characteristics of atmospheric fine and coarse particles

during Taiwan's Lantern Festival, Atmos. Environ., 62 , 256-264, 2012.

U.S. Environmental Protection Agency: EPA-CMB8.2 Users Manual, U.S. EPA,

office of Air Quality Planning and Standards, Research Triangle Park, NC 27711,

2004.

Vassura, I., Venturini, E., Marchetti, S., Piazzalunga, A., Bernardi, E., Fermo, P.,

Passarini, F.: Markers and influence of open biomass burning on atmospheric

particulate size and composition during a major bonfire event, Atmos. Environ., 82 ,

21-225, 2014.

Vecchi, R., Bernardoni, V., Cricchio, D., D'Alessandro, A., Fermo, P., Lucarelli, F.,

Nava, S., Piazzalunga, A., and Valli, G.: The impact of fireworks on airborne

particles, Atmos. Environ., 42, 1121-1132, 2008.

Wang, Y., Zhuang, G.S., Xu, C., and An, Z.S.: The air pollution caused by the burning

of fireworks during the lantern festival in Beijing, Atmos. Environ., 41 , 417-431,

2007.

Watson, J. G., Cooper, J. A., and Huntzicker, J. J.: The effective variance weighting

for least squares calculations applied to the mass balance receptor model, Atmos.

642   Environ., 18, 1347-1355, 1984.

643   Wu, L., Feng, Y.C., Wu, J.H., Zhu, T., Bi, X.H., Han, B., Yang, W.H., and Yang, Z.Q.:

644   Secondary organic carbon quantification and source apportionment of PM10 in

645   Kaifeng, China, J. Environ. Sci., 21, 1353-1362, 2009.

646   Xue, Y.H., Wu, J.H., Feng, Y.C., Dai, L., Bi, X.H., and Li, X.: Source Characterization

647   and Apportionment of PM10 in Panzhihua, China, Aerosol Air Qual. Res., 10,

648   367-77, 2010.

649   Zhang, Y.F., Xu, H., Tian, Y.Z., Shi, G.L., Zeng, F., Wu, J.H., Zhang, X.Y., Li, X., Zhu,

650   T., and Feng, Y.C.: The study on vertical variability of PM10 and the possible

651   sources on a 220 m tower, in Tianjin, China, Atmos. Environ., 45, 6133-6140, 2011.

652   Zhao, P. S., Dong, F., He, D., Zhao, X.J., Zhang, X.L., Zhang, W.Z., Yao, Q. and Liu,

653   H.Y.: Characteristics of concentrations and chemical compositions for PM2.5 in the

654   region of Beijing, Tianjin, and Hebei, China, Atmos. Chem. Phys., 13, 4631–4644,

655   2013a.

656   Zhao, X. J., Zhao, P. S., Xu,, Meng, W., Pu, W. W., Dong, F., He, D. , and Shi, Q. F.:

657   Analysis of a winter regional haze event and its formation mechanism in the North

658   China Plain, Atmos. Chem. Phys., 13, 5685-5696, 2013b.

659   Zheng, M., Salmon, L.G., Schauer, J.J., Zeng, L.M., Kiang, C.S., Zhang, Y.H., and

660   Cass, G.R.: Seasonal trends in PM2.5 source contributions in Beijing, China, Atmos.

661   Environ., 39, 3967-3976, 2005.

662

663

664

Figure captions

666

667

Fig. 1. The averaged concentrations of the chemical species in PM_{10} and $PM_{2.5}$ during the light-firework period and the heavy-firework period.

670

671

Fig. 2. Source profiles ($\mu g/m^3$) and percentage source contributions (%) estimated by PMF for PM_{10} and $PM_{2.5}$.

674

675

Fig. 3. The total influence of fireworks on PM_{10} and $PM_{2.5}$ (%) during the light-firework and heavy-firework periods, estimated by PMF (column chart), and the individual percentage contributions to the total firework impacts estimated by CMB based on Peak Analysis (pie chart).

680

681

Fig. 4. The daily percentage contributions of the total firework impacts to PM_{10} and $PM_{2.5}$, estimated by PMF.

684

685

Fig. 5. Profiles of fireworks (g/g) estimated by PMF for PM_{10} and $PM_{2.5}$, Peak Analysis for PM_{10} and Peak Analysis for $PM_{2.5}$, and the regression plots between these profiles.
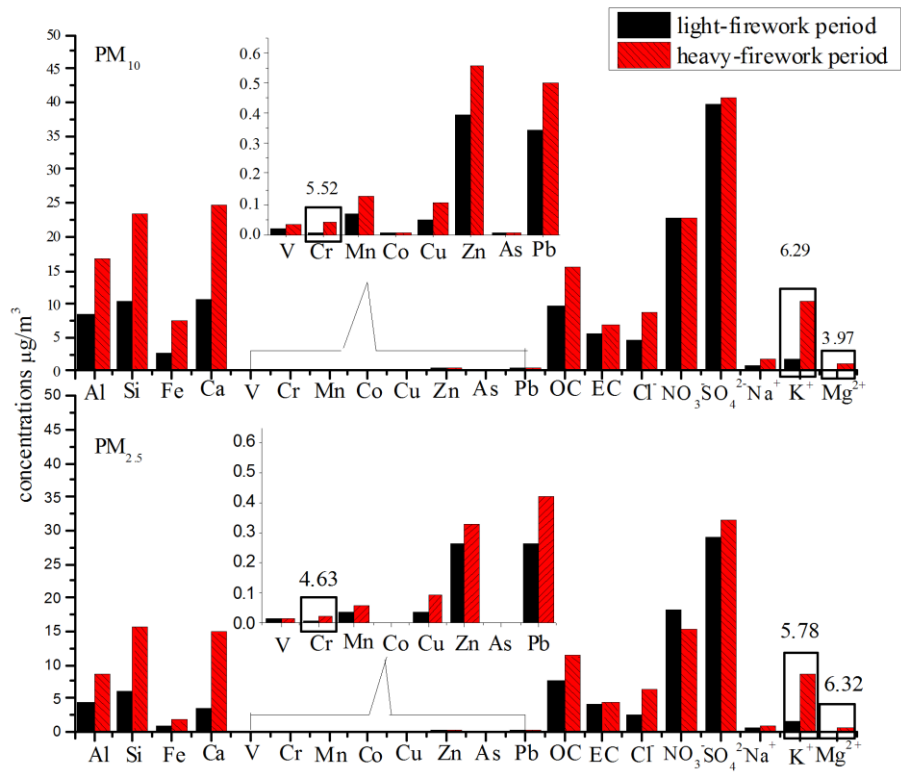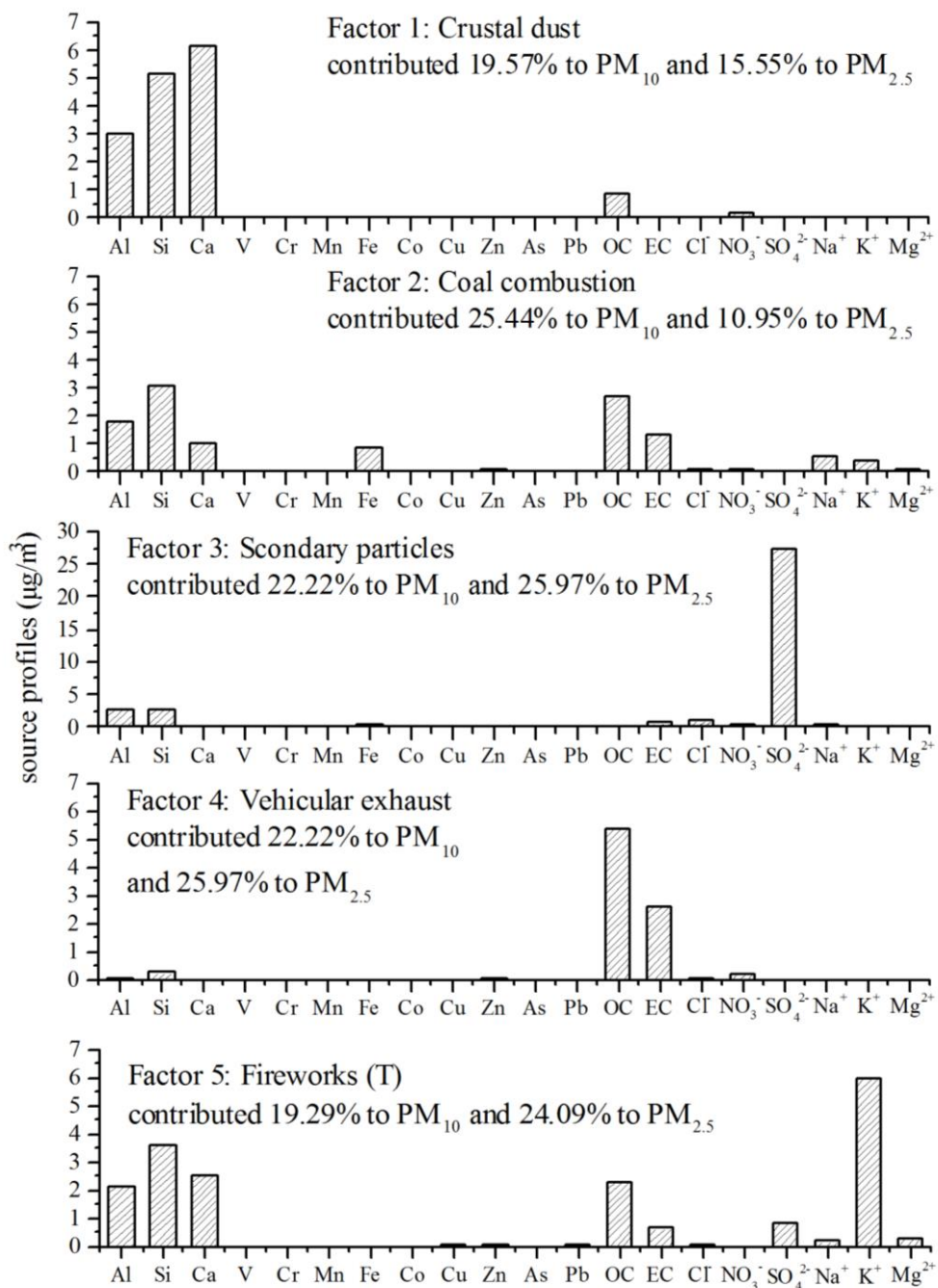
689

Fig. 1

Fig. 2

Factor 1: Crustal dust
contributed 19.57% to PM_{10} and 15.55% to $PM_{2.5}$

Factor 2: Coal combustion
contributed 25.44% to PM_{10} and 10.95% to $PM_{2.5}$

Factor 3: Scondary particles
contributed 22.22% to PM_{10} and 25.97% to $PM_{2.5}$

Factor 4: Vehicular exhaust
contributed 22.22% to PM_{10}
and 25.97% to $PM_{2.5}$

Factor 5: Fireworks (T)
contributed 19.29% to PM_{10} and 24.09% to $PM_{2.5}$

693
694
695

696
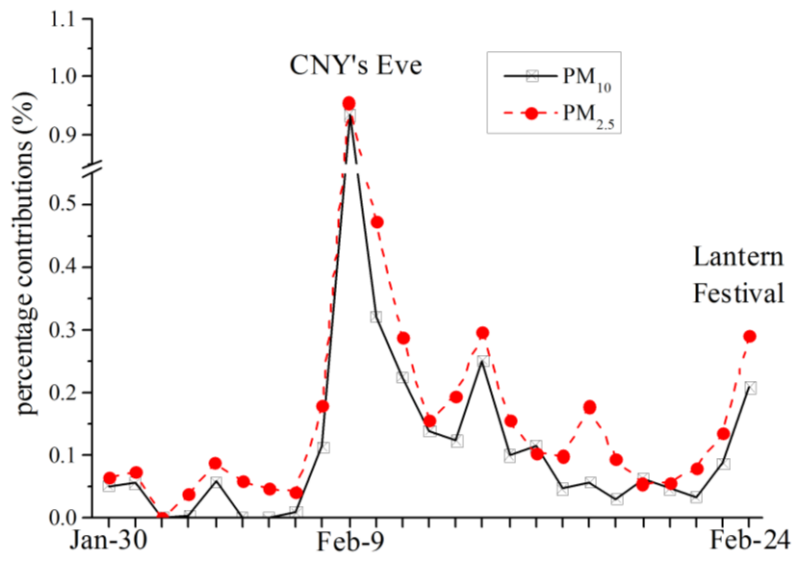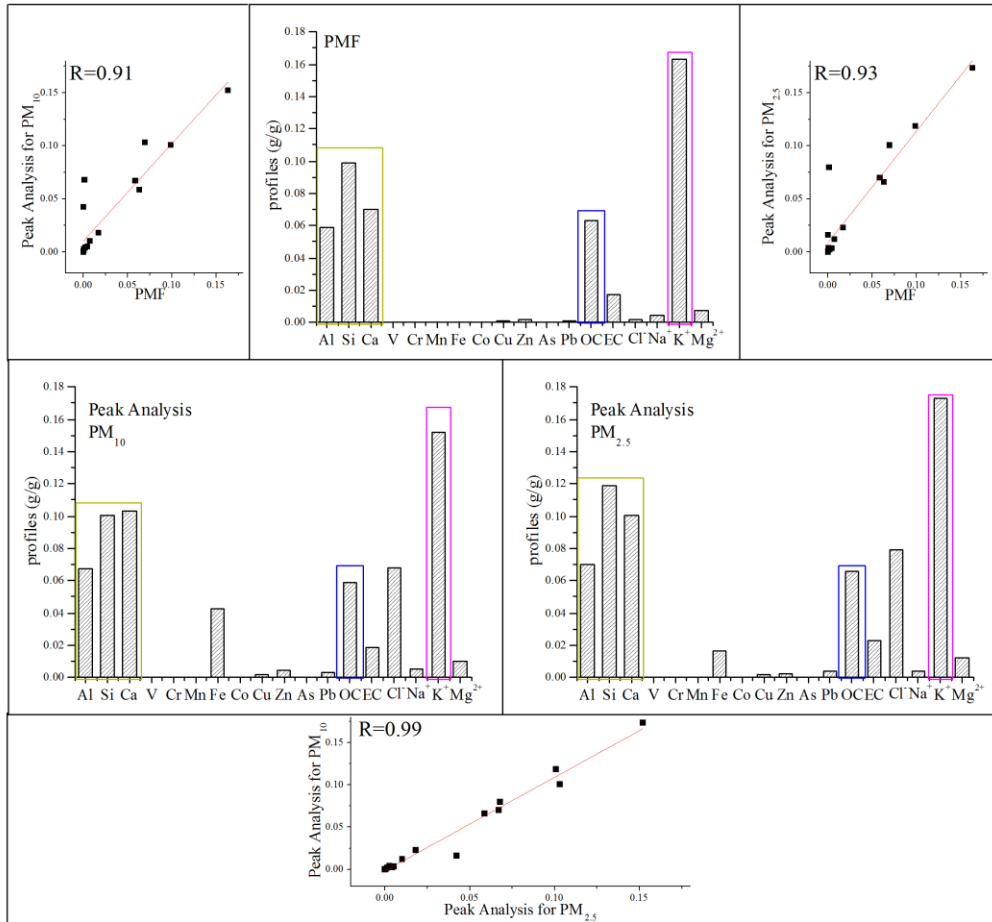697   **Fig. 3**
698

699

Fig. 4

700

701

702

703   **Fig. 5**